SUPPLEMENTARY INFORMATION

Supplementary Table 1	List of oligos used in this work
Supplementary Table 2	List of strains used in this work
Supplementary Table 3	List of plasmids used in this work
Supplementary Table 4	Crystallographic data collection and refinement statistics
Supplementary Table 5	Components of EZ Rich Defined Medium (Teknova)

Supplementary Figure 1	*P. tinctorium* indigo biosynthesis pathway
Supplementary Figure 2	Multiple sequence alignment of UGT amino acid sequences.
Supplementary Figure 3	Michaelis-Menten curves
Supplementary Figure 4	UDP-glucose binding pocket inferred from AtUGT72B1
Supplementary Figure 5	Carbon source affects indigo production
Supplementary Figure 6	Background hydrolysis of indican by wild type vs Δ*bglA E. coli*
Supplementary Figure 7	Panel of *E. coli* β-glucosidase knockouts
Supplementary Figure 8	Detection of indican by LC-MS
Supplementary Figure 9	Water-soluble orange co-produced with indican washes off cotton
Supplementary Figure 10	Indican dyed scarf retains blue color after laundry wash
Supplementary Figure 11	SDS-PAGE of UGTs

Oligo #	Oligo Name	Description	Sequence
1	ET55	Integrate at base 44344920 – forward	CCGGATAAGGAATTCACGCCGCATCCGGCA TCAACAAAGCACTGGCCGATAATTGCAGAC
2	ET56	Integrate at base 44344920 – reverse	AGCTACGGCGCTTTGGCTTGATAACCGGAT AACAACTTGCCTGATCCTTCAACTCAGCAA
3	CA78	Knock out *bglA* – forward	CACCAGCCCAACGATACC
4	DG75	Knock out *bglA* – reverse	ATCAGCAAAACCTCCACGCG

Supplementary Table 1: List of oligos used in this work.

Strain Name	Parent Strain	Accession Number	Description	Antibiotic Marker	Used in Figure
MG1655(DE3)			from Bond-Watts *et al.*, 2011	N/A	S5, S6
MG1655(DE3)Δ*bglA*	1			N/A	3, 4, S6
TMH003	2	MF688770	pT7-FMO-tT7	Kan^R	3, 4, S8
TMH011	2	MF688771	pT7-FMO-PtUGT1-tT7	Kan^R	3, 4, 5, S8, S9, S10

Supplementary Table 2: List of strains used in this work. Gene cassette was integrated into TMH003 and TMH011 at base 44344920 in the *E. coli* genome.

Bond-Watts, B. B., Bellerose, R. J. & Chang, M. C. Y. Enzyme mechanism as a kinetic control element for designing synthetic biofuel pathways. *Nat Chem Biol* 1–6 (2011).

Plasmid Name	Accession Number	Description	Antibiotic Marker	Purpose	Used in Figure
pTMH307	MF688772	pT7-6xHis-PtUGT1-tT7	Amp^R	Purification of PtUGT1	2, S3, S4, S11
pTMH308	MF688773	pT7-6xHis-PtUGT2-tT7	Amp^R	Purification of PtUGT2	S3, S11
pTMH634		pT7-6xHis-PtUGT1_H26A-tT7	Amp^R	Purification of PtUGT1 H26A	S3, S11
pTMH635		pT7-6xHis-PtUGT2_H26A-tT7	Amp^R	Purification of PtUGT2 H26A	S3, S11
pRLP121	MF688774	pT7-6xHis-BglA-tT7	Amp^R	Expression of *B. circulans* glucosidase BglA	3, 5, S10
pTMH561	MF688775	BBa_J23100-BBa_B0034-FMO-tSPY	Kan^R	Constitutive expression of FMO	S5

Supplementary Table 3: List of plasmids used in this work. All plasmids have the ColE1 origin of replication.

BBa_J23100: Anderson, J. C. *et al.* BglBricks: A flexible standard for biological part assembly. *J Biol Eng* **4,** 1 (2010).
tSPY: Chen, Y.-J. *et al.* Characterization of 582 natural and synthetic terminators and quantification of their design constraints. *Nat Meth* **10,** 659–664 (2013).

	PtUGT1:indoxyl sulfate*
Data collection	
Space group	P 21 21 2
Cell dimensions	
a, *b*, *c* (Å)	121, 172.82, 48.41
α, β, γ (°)	90, 90, 90
Resolution (Å)	48.41 - 2.14 (2.216 - 2.14)**
R_{merge}	0.09 (1.52)
$I / \sigma I$	15.58 (0.86)
Completeness (%)	97.97 (84.44)
Redundancy	8.9 (3.9)
Refinement	
Resolution (Å)	2.14
No. reflections	55920
R_{work} / R_{free}	0.23 / 0.25
No. atoms	7131
Protein	6994
Ligand/ion	33
Water	104
B-factors	
Protein	73.81
Ligand/ion	128.8
Water	49.41
R.m.s. deviations	
Bond lengths (Å)	0.002
Bond angles (°)	0.52

*One crystal was used to solve the structure.
**Values in parentheses are for highest-resolution shell.

Supplementary Table 4: Crystallographic data collection and refinement statistics.

Component	Concentration
MOPS	40 mM
Tricine	4.0 mM
Iron Sulfate	0.01 mM
Ammonium Chloride	9.5 mM
Potassium Sulfate	0.276 mM
Calcium Chloride	5×10^{-7} M
Magnesium Chloride	0.525 mM
Sodium Chloride	50 mM
Ammonium Molybdate	3×10^{-9} M
Boric Acid	4×10^{-7} M
Cobalt Chloride	3×10^{-8} M
Cupric Sulfate	10^{-8} M
Manganese Chloride	8×10^{-8} M
Zinc Sulfate	10^{-8} M
Potassium Phosphate Dibasic	1.32 mM
Potassium Hydroxide	1.5 mM
Adenine	0.2 mM
Cytosine	0.2 mM
Uracil	0.2 mM
Guanine	0.2 mM
L-Alanine	0.8 mM
L-Arginine	5.2 mM
L-Asparagine	0.4 mM
L-Aspartic Acid, Potassium Salt	0.4 mM
L-Glutamic Acid, Potassium Salt	0.66 mM
L-Glutamine	0.6 mM
L-Glycine	0.8 mM

L-Histidine HCl H_2O	0.2 mM
L-Isoleucine	0.4 mM
L-Proline	0.4 mM
L-Serine	10 mM
L-Threonine	0.4 mM
L-Tryptophan	0.1 mM
L-Valine	0.6 mM
L-Leucine	0.8 mM
L-Lysine	0.4 mM
L-Methionine	0.2 mM
L-Phenylalanine	0.4 mM
L-Cysteine HCl	0.1 mM
L-Tyrosine	0.2 mM
Thiamine	0.01 mM
Calcium Pantothenate	0.01 mM
para-Aminobenzoic Acid	0.01 mM
para-Hydroxybenzoic Acid	0.01 mM
Dihydroxybenzoic Acid	0.01 mM
Glucose	2 g/L

Supplementary Table 5: Components of EZ Rich Defined Medium (Teknova). Any substitutions made were described in the text.

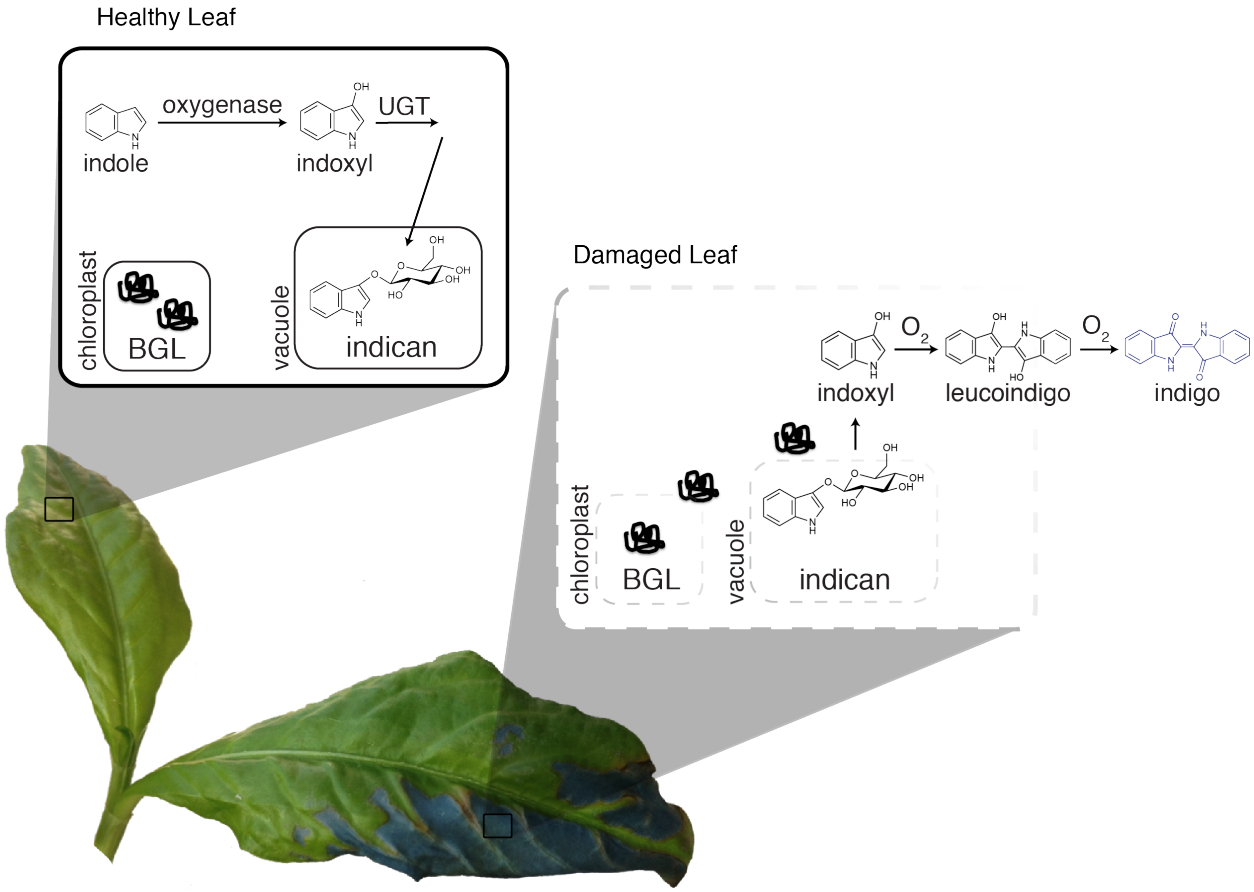

Supplementary Figure 1: *P. tinctorium* indigo biosynthesis pathway. In the indigo plant *P. tinctorium*, the healthy leaf produces and efficiently glucosylates the reactive indoxyl with a glucosyltransferase (UGT) to generate indican, which is stored in the vacuole. Thus, healthy *P. tinctorium* leaves do not show blue coloration. Upon damage to the leaf tissue, induced here by spraying 70% ethanol on the lower right part of the leaf, the vacuole lyses, resulting in indican hydrolysis by a β-glucosidase (BGL) similarly liberated from its chloroplast compartment. The regenerated indoxyl spontaneously oxidizes to form indigo through a leucoindigo intermediate.

Supplementary Figure 2: Multiple sequence alignment of UGT amino acid sequences. Clustal Omega (Sievers *et al.*, 2011) was used to generate a multiple sequence alignment of PtUGT1, PtUGT2, and the closest structurally characterized homolog, UGT72B1 from

Arabidopsis thaliana. Red residues are small and/or hydrophobic; blue residues are acidic; magenta residues are basic; green residues have a hydroxyl, sulfhydryl, or amine. An asterisk (*) denotes a fully conserved residue; a colon (:) denotes a group of strongly similar residues; a period (.) denotes a group of weakly similar residues. PtUGT1 was used for structural studies and indican production in this work. The secondary structure of PtUGT1 (above alignment) was generated by PDBsum (de Beer *et al.*, 2014). Red squares denote residues that contact indoxyl sulfate, based on the crystal structure. Blue squares denote residues that contact UDP-glucose, based on homology to other UGT crystal structures.

Sievers, F. *et al.* Fast, scalable generation of high-quality protein multiple sequence alignments using Clustal Omega. *Mol Syst Biol* **7,** 539 (2011).
de Beer, T. A. P., Berka, K., Thornton, J. M. & Laskowski, R. A. PDBsum additions. *Nucleic Acids Research* **42,** D292–6 (2014).

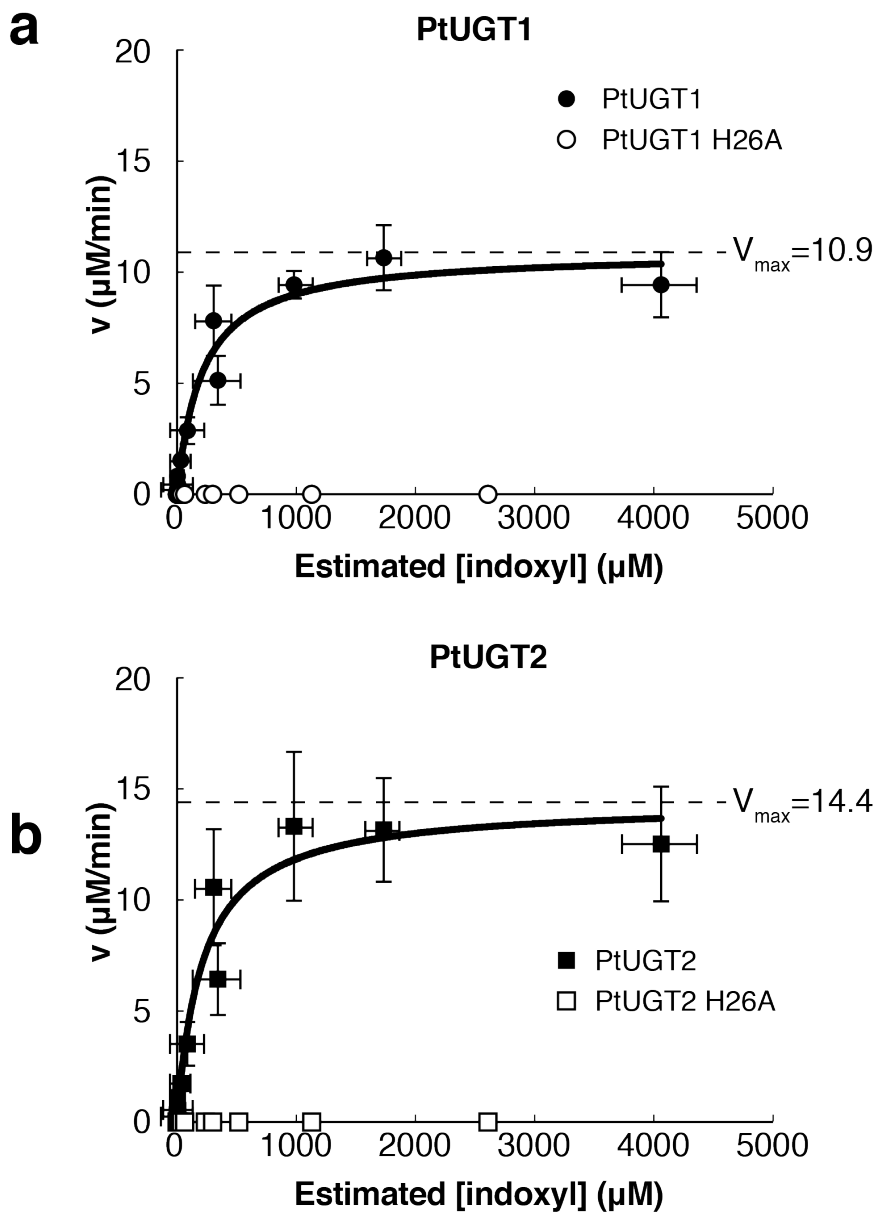

Supplementary Figure 3: Michaelis-Menten curves. PtUGT1 (closed circles) has a k_{cat} of 9.1 ± 0.5 sec^{-1}, and PtUGT2 (closed squares) has a k_{cat} of 12 ± 0.8 sec^{-1}. The corresponding H26A mutants (open circles and squares) show no catalytic activity. The K_M of the enzymes cannot be accurately reported because the concentrations of the indoxyl substrate cannot be determined with high certainty due to the instability of the molecule. Error bars represent the mean ± s.d. of three technical replicates.

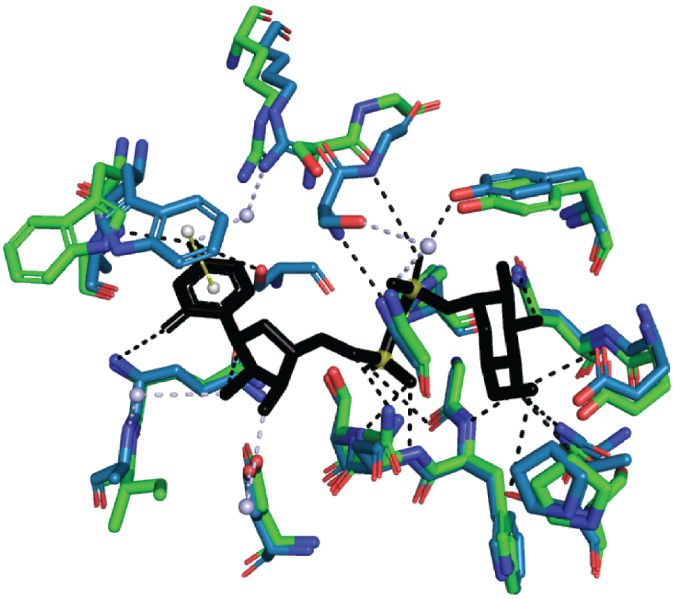

Supplementary Figure 4: UDP-glucose binding pocket inferred from AtUGT72B1. The donor binding site of AtUGT72B1 (PDB ID: 2VCE). The bound UDP-2F-glucose (black), interacting residues (teal) and water molecules (grey) are shown, together with aligned PtUGT1 residues (green), illustrating the putative UDP-glucose binding site of PtUGT1. Interactions are shown as dashed lines (black = hydrogen bond, grey = water bridge, yellow = π-stacking).

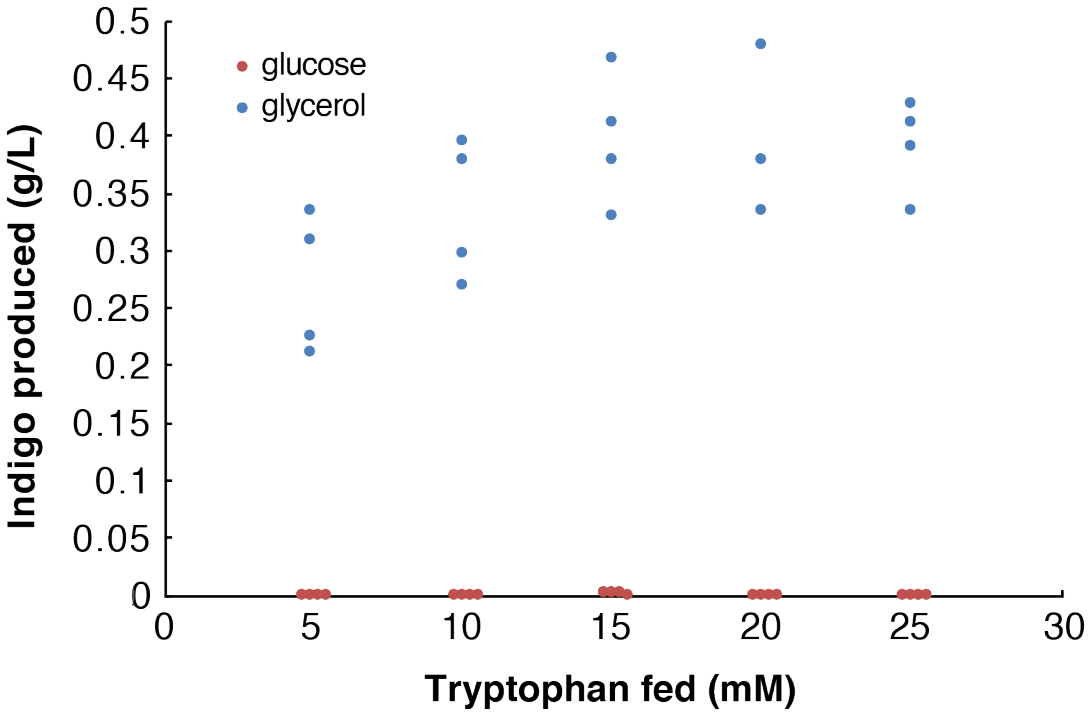

Supplementary Figure 5: Carbon source affects indican production. When cells that constitutively express FMO are fed glucose, they produce significantly less indigo than when fed glycerol. This is most likely due to repression of TnaA expression and activity by glucose. FMO was expressed under a strong constitutive promoter (plasmid pTMH561) in strain background MG1655(DE3). Strains were grown for 24 h in EZ Rich media with 2% w/v glucose or 2% v/v glycerol carbon source. Data points represent independent cell cultures.

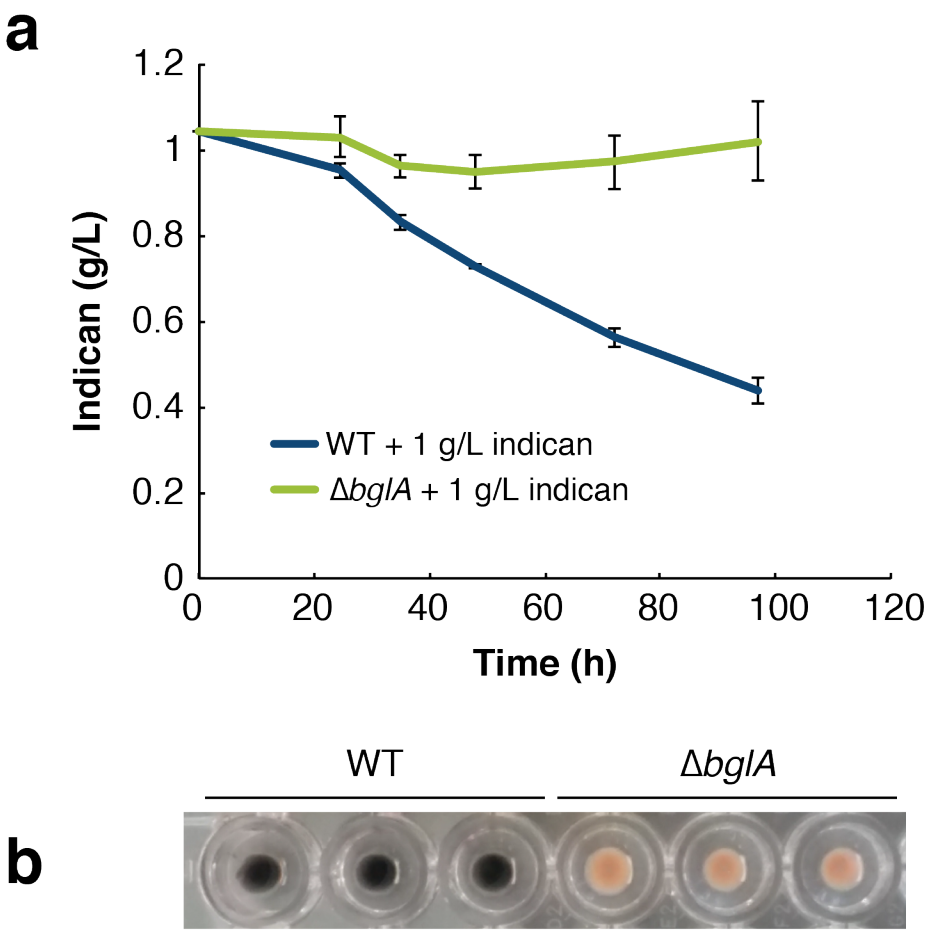

Supplementary Figure 6: Background hydrolysis of indican by wild type vs Δ*bglA E. coli*. a) After 97 h incubation with 1 g/L indican at 37 °C, wild type (WT) MG1655(DE3) *E. coli* grown in EZ Rich media showed considerable indican hydrolysis, whereas the same strain with *bglA* knocked out did not appear to reduce indican titers. Error bars represent the mean ± s.d. of three biological replicates. b) Even after 120 h incubation, very low amounts of indigo were visible in the Δ*bglA* strain (right 3), whereas ample color was observed in the WT strain (left 3).

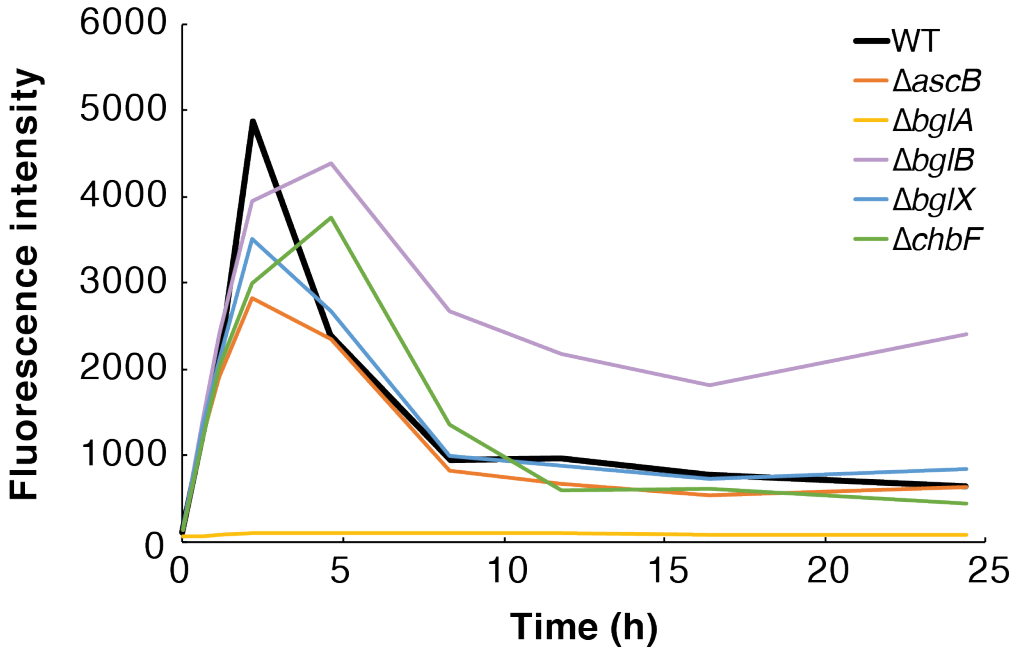

Supplemental Figure 7: Panel of *E. coli* β-glucosidase knockouts. A panel of five *E. coli* β-glucosidase knockouts from the Keio collection (background BW25113; Baba *et al*., 2006) were tested for their ability to hydrolyze 1 mM indican over 24 h. Cultures were grown to saturation and incubated with 1 mM indican in 1x PBS + 20% DMSO. Indoxyl is fluorescent (Gehauf & Goldenson, 1957), and its fluorescence intensity was measured with excitation and emission wavelengths of 410 nm and 490 nm, respectively.

Baba, T. *et al.* Construction of Escherichia coli K-12 in-frame, single-gene knockout mutants: the Keio collection. *Mol Syst Biol* **2,** 473–11 (2006).
Gehauf, B. & Goldenson, J. Detection and estimation of nerve gases by fluorescence reaction. *Anal. Chem.* **29,** 276–278 (1957).

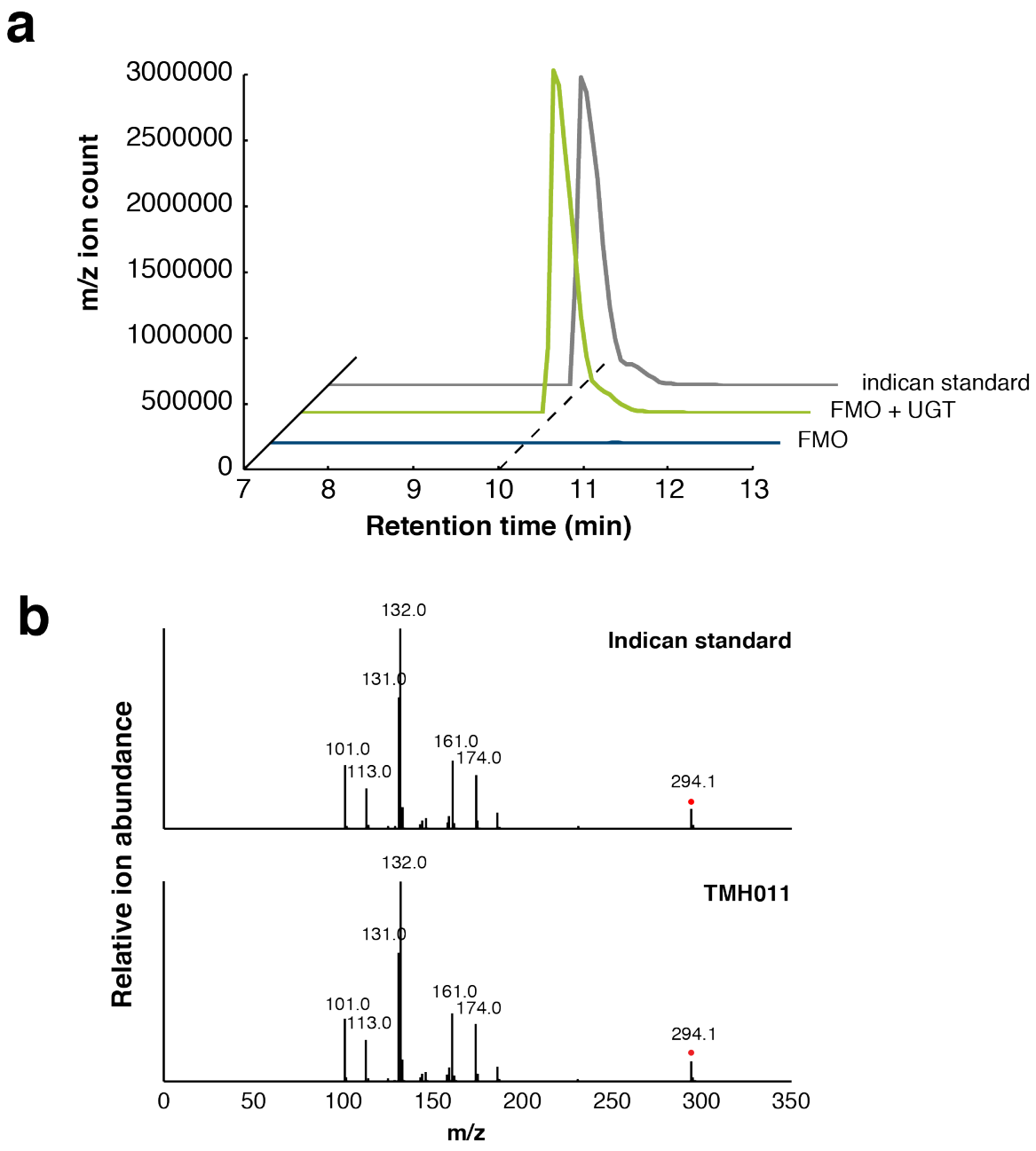

Supplementary Figure 8: Detection of indican by LC-MS. a) Biosynthesized indican made from FMO and UGT has the same retention time as the commercial standard. Indican is only formed in the presence of both FMO and UGT. b) The MS/MS spectra of biosynthesized indican (obtained by collision induced dissociation at 10 V) matches that of the commercial standard. The red dot denotes the parent $[M-H]^-$ ion.

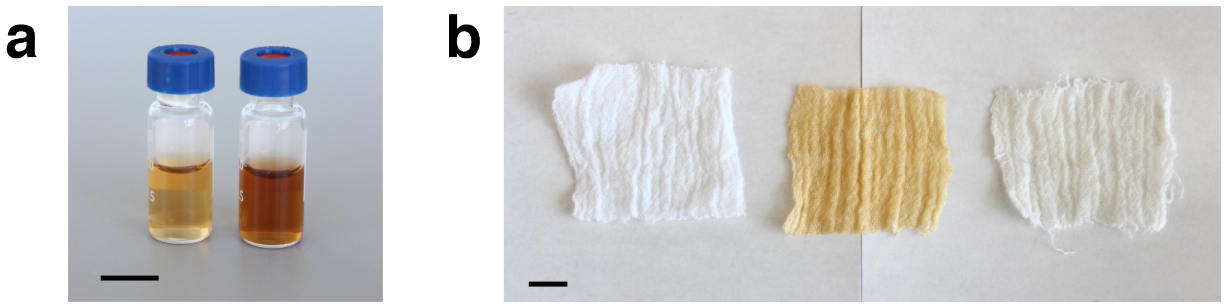

Supplementary Figure 9: Water-soluble orange co-produced with indican washes off cotton. a) An unexpected orange color is produced when FMO is expressed, and the color intensifies when PtUGT1 is co-expressed. Left: supernatant of TMH003 24h after induction with IPTG. Right: supernatant of TMH011 24h after induction with IPTG. b) The media shows an orange color when FMO and PtUGT1 are expressed, but it washes out of fabric. Left: white cotton gauze with EZ Rich media applied. Middle: white cotton gauze with indican broth applied (see “Indican production in bioreactor” in Online Methods). Right: gauze fabric applied with indican broth was allowed to air dry, and it was then washed in a cold-water laundry cycle with All detergent. Scale bars, 1 cm.

Supplementary Figure 10: Indican dyed scarf retains blue color after laundry wash. Although some surface-adsorbed indigo is lost after washing (compare to Fig. 5b), much of the blue color is retained. Scale bar, 5 cm.

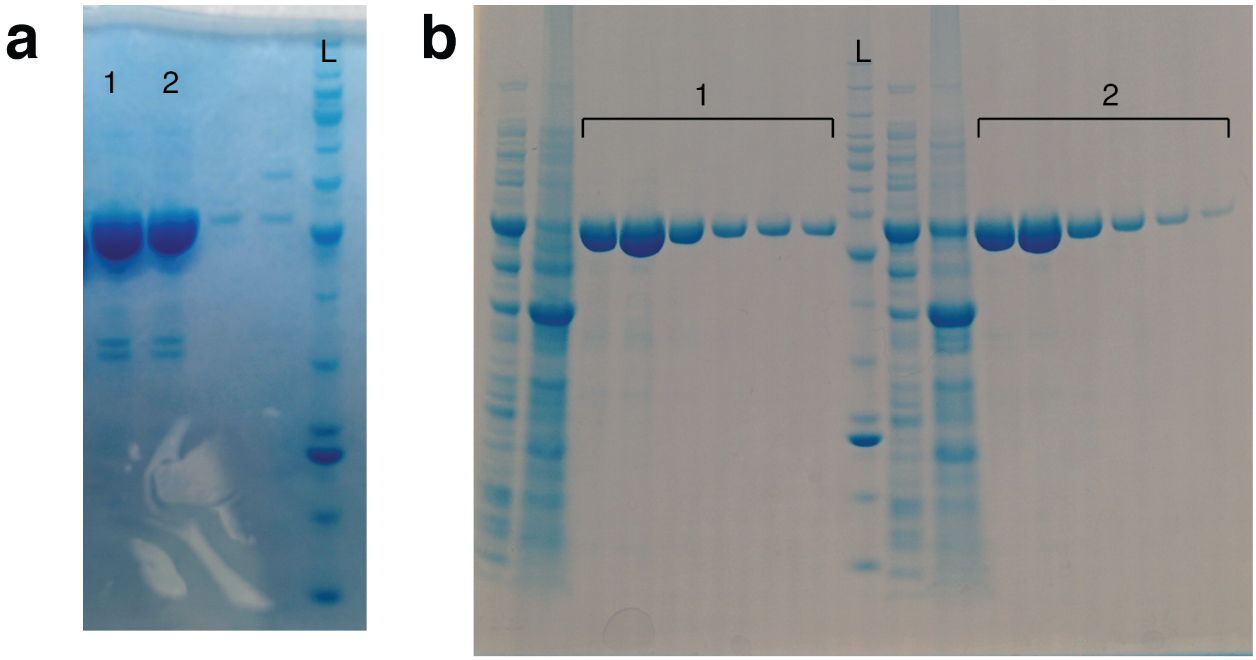

Supplementary Figure 11: SDS-PAGE of UGTs. The proteins show high purity with a strong band at 52 kDa on a NuPAGE Novex 4-12% Bis-Tris Protein Gel (Life Technologies). a) Lane 1 is pTMH307, lane 2 is pTMH308, lane L is BenchMark Protein Ladder. b) Lanes in section 1 are pTMH634 fractions, lane L is BenchMark Protein Ladder, lanes in section 2 are pTMH635 fractions.